

## Local Structural Distortions in InAsP/InP Strained Layer Superlattices

S. Pascarelli<sup>\*(1)</sup>, F. Boscherini<sup>\*\*</sup>, C. Lamberti<sup>\*\*\*</sup> and S. Mobilio<sup>\*\*\*\*</sup>

\* *Istituto Nazionale per la Fisica della Materia, Via dell'Acciaio 139, 16152 Genova, Italy*

\*\* *Istituto Nazionale di Fisica Nucleare, Laboratori Nazionali di Frascati, CP13, 00044 Frascati, Italy*

\*\*\* *Dipartimento di Chimica IFM, Università di Torino, Via P. Giuria 7, 10148 Torino, Italy*

\*\*\*\* *Dipartimento di Fisica, Università "Roma Tre", Via della Vasca Navale 84, 00146 Roma, Italy*

**Abstract:** The local structure around As in thin  $\text{InAs}_x\text{P}_{1-x}$  strained layers in  $\text{InAs}_x\text{P}_{1-x}/\text{InP}$  superlattices has been probed by fluorescence detected XAFS as a function of composition, and compared to that found in unstrained, bulk samples of similar composition. Contributions up to the third coordination shell around As were clearly visible in the spectra and were analyzed taking into account the major multiple scattering contributions. Differences in the local structure between the thin strained films and the bulk alloys are expected to arise from tetragonal strain due to epitaxy with the substrate. Results are consistent with a picture in which long range order in the strained layers is mainly achieved via bond angle distortions, as first shell bond distances follow the measured and theoretically predicted values of the bulk alloys. Evidence of the influence of tetragonal distortion on the local structure appears in further coordination shells.

### 1. INTRODUCTION

The atomic level structure in pseudobinary semiconductor alloys of the type  $\text{AB}_x\text{C}_{1-x}$  (or  $\text{A}_x\text{B}_{1-x}\text{C}$ ) has been extensively studied and is now well understood [1-4]. On the other hand, very little is still known on the local atomic structure in strained thin films of pseudobinary semiconductors. A strained epilayer may be grown on a substrate having a different lattice constant, provided its thickness is kept below a certain critical value. In this case, the strain due to the lattice mismatch is elastically accommodated by a tetragonal distortion of the grown layer (pseudomorphic growth). The question of how the distortion of the unit cell of the strained layer influences the local atomic structure is still open and very few theoretical studies related to this problem are found in the literature [5]. Local atomic investigations on similar strained semiconductor thin films are mainly limited to first shell structural information, and report both strained and unstrained bond lengths [6-10].

Besides the fundamental interest in determining the strain accommodation mechanisms in these materials, a strong motivation to obtain a local atomic description of the strained layer structure arises from semiconductor technology, searching for useful hints on strain incorporation which affects pseudomorphic growth. From an applicative point of view, the structural characterization of  $\text{InAs}_x\text{P}_{1-x}/\text{InP}$  interface layers in  $(\text{InAs}_x\text{P}_{1-x}/\text{InP})_N$  superlattices is of particular interest in the context of optimization of InP/InGaAs Multi Quantum Well heterostructures [11].

This paper reports a XAFS investigation of the first three coordination shells around As in  $(\text{InAs}_x\text{P}_{1-x}/\text{InP})_N$  strained layer superlattices and in unstrained bulk samples of similar composition. The global picture obtained by XAFS on the local environment of As in the strained layers will be completed, in a separate paper [12], by information regarding the average displacement, along the growth direction, of As atoms in the unit cell, obtained through a parallel X-ray standing waves investigation on the samples.

Differences in the local structure between the thin strained films and the bulk alloys are expected to arise from tetragonal strain due to epitaxy with the substrate. A simple model for the thin  $\text{InAs}_x\text{P}_{1-x}$  layers subject to tetragonal strain predicts, in the  $x = 1$  limit, a  $0.02 \text{ \AA}$  contraction of the nearest neighbor bond and a  $0.03 \text{ \AA}$  contraction of the measured second shell distances. Since these quantities are upper limits, the effect on the local structure due to tetragonal distortion in the  $\text{InAs}_x\text{P}_{1-x}$  thin layers is indeed at the limit of detectability. To record high quality spectra in such extremely low As containing samples, a very high photon flux as well as an adequate fluorescence detection system, which could efficiently separate the As fluorescence from the strong elastically scattered background arising from the thick substrate, was needed. Moreover, for the first time a full multiple scattering analysis of the XAFS spectra was performed to get a reliable structural picture beyond the first shell on these strained semiconductor superlattices.

### 2. EXPERIMENTAL

The superlattices (SL) consist of 50 to 1000 layers of  $\text{InAsP}(\approx 10 \text{ \AA})/\text{InP}(\approx 50 \text{ \AA})$  epitaxially grown on InP (100) by LP-MOCVD. All samples have been thoroughly characterized with more conventional techniques such as HRXRD, HRTEM, and 4K Fourier-transform photoluminescence, and relative simulations [11,13]. The measurements provided information on the crystalline quality of the superlattices, indicating that some were perfect, while others had less abrupt interfaces and lower period reproducibility. The SL period  $\Delta$ , thickness and As content of the ternary layers,  $t_{\text{InAsP}}$  and  $x$  respectively, and perpendicular mismatch between ternary layer and substrate,  $\epsilon_{\perp} = (a_{\perp} - a_{\text{InP}})/a_{\text{InP}}$ , were obtained and are reported in Table I. Six bulk  $\text{InAs}_x\text{P}_{1-x}$  samples were also prepared as standards for comparison: three polycrystalline samples ( $1.0 \geq x \geq 0.6$ , referred

<sup>(1)</sup> Present address: GILDA CRG, ESRF, BP. 220, 38043 Grenoble cedex, France.

to as B1, B2 and B3) grown on Al substrate, and three unstrained "bulk" samples ( $0.5 \geq x \geq 0.1$ , referred to as B4, B5 and B6) epitaxially grown on InP (100), with a thickness greater than the critical thickness.

EXAFS measurements at the As K-edge were performed at the GILDA beamline at the ESRF [14]. The monochromator operated with Si (311) crystals in a dynamical sagittal focusing mode [15]. Energy resolution and flux were approximately 1.2 eV and  $10^9$  photons/sec on the sample, with a focal image of about 1 mm<sup>2</sup>. Harmonic rejection was performed by detuning the two crystals. The EXAFS measurements were performed in the transmission mode on the bulk samples on Al and in the fluorescence mode on all the others, using a hyperpure Ge detector to discriminate the As K $\alpha$  fluorescence yield from the elastically scattered background. The polarization vector of the beam was directed along the (110) crystallographic direction. Measurements on all samples except H2 were performed at T = 77 K.

### 3. RESULTS

The data analysis was performed using the GNXAS software package [16]. In our case the calculated signals included in the model  $\chi(k)$  were: a) all the single scattering (SS) contributions relative to the first three coordination shells around As and b) the important multiple scattering (MS) contributions. The inclusion of MS contributions in this system has proved to be essential for a correct determination of the structural parameters relative to the second shell As-As distance. In fact, the most important MS path, that arising from the As-In-As triangle, adds a non negligible signal with a frequency intermediate between those relative to the second and third shell SS paths. The fitting parameters were: a) for the first and third shell: As-In bond distance and mean square relative displacement:  $R_1, \sigma_1^2, R_3, \sigma_3^2$ ; b) for the second shell: As coordination,  $N_{AS}$ ; As-In-As and As-In-P bond angles  $\theta_{As-As}$  and  $\theta_{As-P}$ , from which As-As and As-P distances were calculated; and one average mean square relative bond angle displacement,  $\sigma_\theta^2$ . Total coordination numbers were assumed equal to nominal values in the zincblende structure [1]. Other structural parameters which are involved in the  $\chi(k)$  signal only through MS paths, such as  $R_{InP}$  and  $\theta_{In-In}$  were fixed to their nominal values in the binary compounds, i.e. 2.54 Å and 109.47° respectively. The values of  $E_0$  and of  $S_0^2$  were obtained from the best fit of the spectrum relative to sample B1.

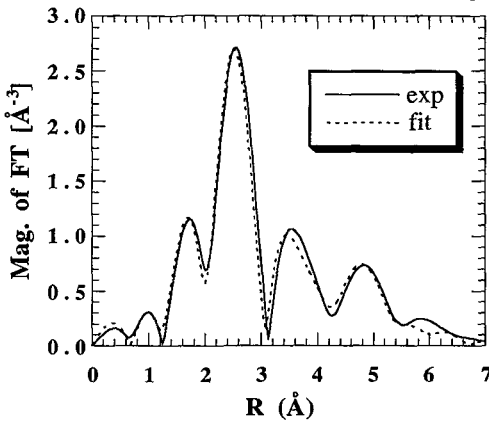


**Figure 1:** Comparison between the FT of the experimental and model  $k^2\chi(k)$  relative to sample H5. The FT is performed in the k range 3-10 Å<sup>-1</sup>.

### 4. DISCUSSION

In bulk  $InAs_xP_{1-x}$ , As and P atoms share the same sublattice and, as is the general case in pseudobinary semiconductor alloys, the lattice parameter  $a_{InAsP}$  follows quite closely Vegard's Law, i.e. varies linearly with x, from  $a_{InAs}$  to  $a_{InP}$ . As shown in Fig. 2, values of first, second and third shell distances obtained on the series of bulk samples are in agreement with the generally accepted picture of the structure of pseudobinary semiconductor alloys: a) the bond lengths have almost the same value as in pure compounds, thus nearest neighbor distances display a bimodal distribution and b) on the chemically disordered

**Table 1:** Superlattice characterization obtained with HRXRD and HRTEM. Columns 3 through 7 contain: ternary layer As content and thickness, SL period, number of periods, and perpendicular mismatch between strained layer and substrate.

sample	code	x	t(Å)	$\Delta(\text{Å})$	N	$\epsilon_{\perp}(\%)$
H1	141	0.59	10	91	50	4.0
H2	137	0.33	10	90	50	2.3
H3	183	0.24	13	63	360	1.6
H4	157	0.20	15	93	50	1.4
H5	182	0.19	18	53	300	1.3
H6	114	0.17	10	60	1000	1.2
H7	032	0.05	10	77	100	0.3

Due to spurious signals on a few spectra, caused by small elastic scattering not efficiently filtered by the detection system, the fittings had to be limited to a maximum energy of  $E=12250$  Å (corresponding to a k range 0 - 10 Å<sup>-1</sup>).

An example of fit is illustrated in Figure 1, where the Fourier Transforms (FT) of the experimental and model  $k^2\chi(k)$  functions relative to sample H5 are compared. The contributions arising from the first three coordination shells around As are clearly visible and are fairly well reproduced by the model. For all samples, the first peak with its small shoulder towards lower distances, is found to be well reproduced by the contribution of 4 In atoms. As for the second peak, the fit has been obtained using two signals due to second shell As and P atoms respectively. Finally, the third peak was reproduced by an average signal due to 12 In atoms bonded to the second shell As (or P) atoms in an As-In-As (or P)-In bond sequence. The best fit  $\sigma_3^2$  values are consistent with the coexistence of the two different third shell distances. Moreover, larger bond angle disorder has been detected in the thin layers compared to the bulk, in agreement with the expected effect of tetragonal distortion. The best fit values of bond distances relative to both bulk and SL samples are plotted in Figures 2a-d.

sublattice the distances approach the Virtual Crystal Approximation (VCA) limit (i.e. interatomic distances scale linearly with the lattice parameter) [1,2,17,18]. Different models have been developed to explain these results [3, 4, 17, 19]. The physical mechanism at the origin of the revealed bond rigidity is related to the fact that minimization of distortion energy in semiconductor alloys is obtained preferentially through bond angle distortions, as bond bending force constants are considerably smaller than bond stretching ones. It is interesting to compare our results on the bulk alloys with recent theoretical estimates [4] on the first and second shell bond distortions expected in bulk pseudobinary alloys. As for the third shell, we underline that no experimental work nor theoretical predictions on similar systems has been found by the authors. The third shell around As is expected to originate from the contribution of two distinct distances for the As-In-As-In and the As-In-P-In bonds respectively. Based on an extrapolation of the above mentioned calculations, we estimate average third shell distance values. From Fig. 2a-d we see that these predictions are in excellent agreement with our findings.

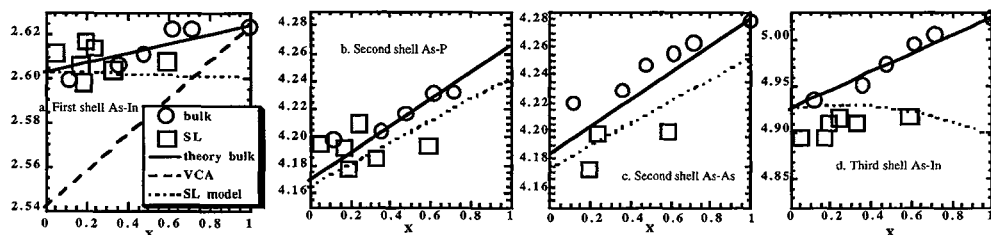


**Figure 2:** Comparison between best fit bond lengths and theoretical predictions for bulk [4] and superlattice (SL) samples.

Results relative to the superlattices are, globally, similar to those found for the bulk alloys, with the exception of third shell distances which are quite smaller than those found for bulk alloys of similar composition. Differences in the structure of the thin strained layers with respect to the bulk samples are expected to arise mainly from tetragonal distortion of the unit cell. Therefore sample H1, reported having the largest mismatch value ( $\epsilon_{\perp} = 4\%$ ), is expected to show the greatest deviations in local structure. In the  $x=1$  limit, i.e. an InAs layer grown pseudomorphically on InP, the environment of As is expected to change as follows: the first and third shell As-In distances contract from the values in the bulk to  $\sqrt{(3+2\epsilon_{\perp}+\epsilon_{\perp}^2)} \cdot a_{\text{InP}}/4$  and  $\sqrt{(11+2\epsilon_{\perp}+\epsilon_{\perp}^2)} \cdot a_{\text{InP}}/4$  respectively. The second shell splits into two subshells: the 4 As atoms on the epitaxial plane lie at a distance of  $\sqrt{2} \cdot a_{\text{InP}}/2$  while the other 8 are at  $(\sqrt{2+2\epsilon_{\perp}+\epsilon_{\perp}^2}) \cdot a_{\text{InP}}/2$ . In the absence of theoretical estimates for bond lengths in strained layers we have compared our results with values calculated using a very simple model, obtained by extending this picture to the general case  $x < 1$ . The underlying hypothesis are: a) the growth in the thin ternary layers is pseudomorphic, and b) in the absence of tetragonal distortion of the unit cells, the local structure in the ternary layer is identical to that in the bulk. The model includes corrections for the different sensitivity of fluorescence detected XAFS to second shell distances in and out of the epitaxial plane. The predicted values (dotted line in Fig. 2a-d) are in good agreement with the experimental data.

To conclude, bond distance values relative to the first three coordination shells around As in thin strained  $\text{InAs}_x\text{P}_{1-x}$  layers have been obtained by performing a complete MS analysis of the EXAFS spectra. The comparison with unstrained alloys of similar composition shows that strain due to alloying is accommodated mainly through bond angle distortions, as first shell bond lengths follow the measured and predicted values relative to the bulk samples. Evidence of the influence of tetragonal distortion on the local structure starts appearing in second shell distance values, and becomes quite strong in third shell distance values.

## References

- [1] Mikkelsen J.C. and Boyce J.B., Phys. Rev. Lett. **49** (1982) 1412-1415
- [2] Balzarotti A., Czyzyk M., Kisiel A., Motta N., Podgorny M., Zimnal-Starnawska M., Phys. Rev B **30** (1984) 2295-2298
- [3] Martins J.L. and Zunger A., Phys. Rev. B **30** (1984) 6217-6220
- [4] Cai Y. and Thorpe M.F., Phys Rev B **46** (1992) 15872-15878; ib.15879-15886
- [5] Bonapasta A. A. and Scavia G., Phys. Rev. B **50** (1994) 2671-2674
- [6] Lamberti C., Bordiga S., Boscherini F., Pascarelli S., and Schiavini G.M., Appl. Phys. Lett. **64** (1994) 1430-1432
- [7] Oyanagi H., Takeda Y., Matsushita T., Ishiguro T., Yao T., Sasaki A. Superlattices and Microstructures **4** (1988) 413-416
- [8] Kuwahara Y., Oyanagi H., Shioda R., Takeda Y., Yamaguchi H. and Aono M., Jpn. J. Appl. Phys. **33** (1994) 5631-5635
- [9] Tabuchi M., Kumamoto T., Takeda Y., J. Appl. Phys. **77** (1995) 143-145
- [10] Proietti M.G., Turchini S., Garcia J., Lambie G., Martelli F. and Prosperi T., J. Appl. Phys. **78** (1995) 6574-6583
- [11] Lamberti C., Computer Physics Communications **93** (1996) 53-81; ib. 82-119 and references therein
- [12] Boscherini F., Pascarelli S., Lamberti C., Gastaldi L., De Martino R., Calicchia P., Comin F., these proceedings
- [13] Antolini A., Francesio L., Gastaldi L., Genova F., Lamberti C., Lazzarini L., Papuzza C., Rigo C., Salviati G., J. Cryst. Growth **127** (1993) 189-193
- [14] Pascarelli S., D'Acapito F., Antonoli G., Balerna A., Boscherini F., Cimino R., Dalba G., Fornasini P., Licheri G., Meneghini C., Rocca F., and Mobilio S., ESRF Newsletter **23** (1995) 17-19
- [15] Pascarelli S., Boscherini F., D'Acapito F., Hrdy J., Meneghini C., and Mobilio S., J. Synch. Rad **3** (1996) 147-155
- [16] Filipponi A., Di Cicco A., Natoli C.R., Phys. Rev. B **52** (1995) 15122-15134; Filipponi A. and Di Cicco A., ib. 15135-15149
- [17] Mikkelsen J.C. and Boyce J.B., Phys. Rev. B **28**, (1983) 7130-7140
- [18] Wu Z., Lu K., Wang Y., Dang J., Li H., Li L., Fang Z., Phys. Rev B **30** (1993) 8694-8700
- [19] Letardi P., Motta N., and Balzarotti A., J. Phys C **20** (1987) 2853-2884